IOP Publishing Metrologia
Metrologia **49** (2012) S156–S160 doi:10.1088/0026-1394/49/2/S156

Photon number statistics of NV centre emission

W Schmunk[1], M Gramegna[3], G Brida[3], I P Degiovanni[3], M Genovese[3], H Hofer[1], S Kück[1], L Lolli[3], M G A Paris[4], S Peters[1], M Rajteri[3], A M Racu[1], A Ruschhaupt[2], E Taralli[3] and P Traina[3]

[1] Physikalisch-Technische Bundesanstalt Braunschweig, Bundesallee 100, 38116 Braunschweig, Germany
[2] Institut für Theoretische Physik, Leibniz Universität Hannover, Appelstr. 2, 30167 Hannover, Germany
[3] Istituto Nazionale di Ricerca Metrologica INRIM, Strada delle Cacce 91, 10135 Torino, Italy
[4] Dipartimento di Fisica, Università degli Studi di Milano, 20133 Milano, Italy

E-mail: silke.peters@ptb.de

Received 18 September 2011, in final form 7 December 2011
Published 2 March 2012
Online at stacks.iop.org/Met/49/S156

Abstract
Optical sources that deterministically produce single photons with a high suppression of multi-photon emission and a negligible background component are promising candidates for standard sources for quantum metrology, quantum communication and foundations of quantum mechanics. In this paper, the photon number distribution of non-classical light emitted by nitrogen vacancy (NV) centres in nano-diamonds is studied by three different experimental techniques. The photon number resolving transition edge sensor (TES) detector and the On/Off detection method are applied to determine the diagonal elements of the optical density matrix. From the data measured by the two methods the second order correlation function at time delay zero is calculated and compared with the $g^2(0)$-values obtained by Hanbury Brown–Twiss (HBT) interferometric measurements. Among the $g^2(0)$-values evaluated with the three techniques, we found good agreement in the results for a single photon emitter with a $g^2(0)$-value close to zero and a multi-photon source with a $g^2(0)$-value of approximately 0.5.

(Some figures may appear in colour only in the online journal)

1. Introduction

One key element of quantum technologies is the ability to prepare true single photon states, whose applications range from quantum key distribution (QKD), yielding high photon rates without diminishing communication security by multi-photon events that an eavesdropper could exploit [1–3], linear optics quantum computation [4] to quantum metrology [5–7] and studies on foundations of quantum mechanics [8]. In particular, in optical quantum metrology there is increasing interest in the preparation of such states for redefining the candela unit in terms of single photon counting [9, 10].

In practice the use of attenuated laser light with Poissonian statistics can represent a reasonable compromise for QKD. But for other applications it could be only an inadequate solution, e.g. metrological studies require the use of a non-classical light beam of a single photon source (SPS). On the other hand, present SPSs are imperfect, as witnessed by their non-vanishing autocorrelation $g^2(0)$-value at zero time delay, implying residual multi-photon emission [11], and the presence of a significant vacuum component.

The ability to resolve the photon number distribution of light pulses can be achieved by a detector with true photon number resolution such as the transition edge sensor (TES) device [11–13] or by combining single photon detectors through temporal or spatial multiplexing [11, 14]. Alternative methods are e.g. the On/Off detection technique [15, 16] or homodyne detection [17].

In this work we report on, to the best of our knowledge, the first analysis of the photon number distribution of light emitted by nitrogen vacancy (NV) centres in nano-diamonds. The investigated solid state vacancies provide photon rates up to 10^6 counts per second (cps) together with an excellent photo-stability at room temperature, which makes them useful for metrological characterization of single photon detectors in the appropriate spectral range. In order to assess the accuracy of our analysis, we determine the diagonal elements of the optical density matrix by a TES detector and through the On/Off

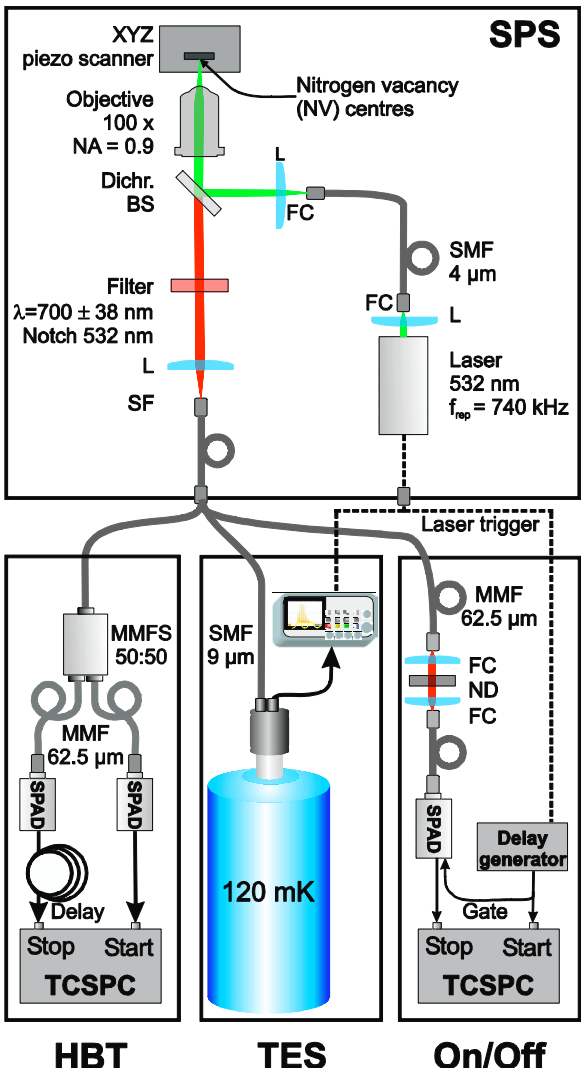

Figure 1. Experimental setup of the SPS based on NV centres used for the three different measurement techniques: HBT, TES measurements, On/Off detection (FC: fibre coupler, dichr. BS: dichroic beamsplitter, L: lens, SF: spatial filter, SMF: single mode fibre, MMF: multi mode fibre, MMFS: multi mode fibre splitter, ND: neutral density filter).

detection method, which is assisted by maximum likelihood estimation, and compare the values with those obtained by the second order correlation function at zero time delay from Hanbury Brown–Twiss (HBT) interferometric measurements.

2. Experiment

Our source of non-classical light is the emission of pulsed laser excited single NV centres in nano-crystalline diamonds, which are addressed using a scanning confocal microscope setup [11], shown in figure 1. To generate a proper Gaussian mode, the irradiating laser light at 532 nm generated by a mode-locked Nd : YVO_4 laser (LYNX-SHG, Time Bandwidth) is first coupled into a single mode fibre and finally into the microscope objective, see figure 1. A pulse picker device (AOM Driver Model 64388.5-SYN-10.5-1, Gooch and Housego) reduces the initial laser repetition rate by a factor of ten to $f_{\mathrm{rep}} = 740\,\mathrm{kHz}$. The fluorescence light of the NV centres is collected by the same objective (NA = 0.9), which focuses the laser beam on the nano-crystals and is coupled into an optical fibre that acts as a spatial filter (SF) to ensure that only light from a narrow focal volume is observed. To suppress the excitation laser line as well as to narrow the fluorescence spectrum centred at $\lambda_c = 700\,\mathrm{nm}$, the emitted fluorescence light passes a 532 nm Notch filter (Melles Griot), a 560 nm long pass filter and a $(700 \pm 38)\,\mathrm{nm}$ band pass filter. In our setup, schematically shown in figure 1, it is possible to connect the fibre output of the SPS to different experiments, e.g. HBT interferometer, On/Off setup, etc.

To measure the second order correlation function $g^2(t)$ of different NV centres, the light coming from the SPS is sent to a HBT interferometer consisting of an optical fibre splitter and two fibre-coupled silicon single photon avalanche detectors (Si-SPAD) (SPCM-AQR-14, Perkin Elmer). Their signals are recorded by a time-correlated single photon counting (TCSPC) module (PicoHarp 300, PicoQuant) for durations of 100 s.

The photon number distribution of different NV centres has been experimentally measured by a TES detector fabricated at INRIM. This type of detector is a microcalorimeter based on a superconducting thin film working as a very sensitive thermometer, which is able to discriminate several photons per pulse. The employed TES consists of a bi-layer of superconducting Ti on Au films [19] with a transition temperature $T_c = 121\,\mathrm{mK}$ and a transition width $\Delta T_c = 2\,\mathrm{mK}$. The fluorescence light coming from the SPS is sent through a 9 µm core single mode optical fibre to the detector surface. Using a stereomicroscope, the fibre is aligned to the $20\,\mu\mathrm{m} \times 20\,\mu\mathrm{m}$ active area of the TES device [12]. Since the SPS is operated at the laser repetition rate of 740 kHz, which is higher than the maximum TES count repetition rate ($f_c \sim 200\,\mathrm{kHz}$), the oscilloscope acquiring the data is armed by the current trigger event only if the TES device has not detected photons at the previous laser trigger. Therewith, it can be ensured that the measurements are not affected by a pulse pile-up induced by the laser repetition rate. The TES read-out is performed by a dc-SQUID (superconducting quantum interference device) current sensor producing a current pulse, whose amplitude is proportional to the absorbed energy, and if the single photon energy is known, also to the number of absorbed photons. The energy resolution of the TES is $\Delta E = 0.41\,\mathrm{eV}$ at 690 nm. The SQUID output is addressed to an oscilloscope (400 MHz, Le Croy) performing the data acquisition, first elaboration and the storage of the data. More details about the characterization and the operation of the TES detector are published in [12, 13].

On/Off detection measurements are performed using a conventional non-photon-number-resolving SPAD (SPCM-AQR-14, Perkin Elmer) sending a logic output signal while one or more photons impinge on its surface. The probability of 'no-click' events for a quantum efficiency η_v is given by

$$\rho(\eta_v) = \sum_n (1 - \eta_v)^n \rho_n, \qquad (1)$$

where ρ_n is the probability of finding n photons. This probability increases with diminishing detection efficiency η_v

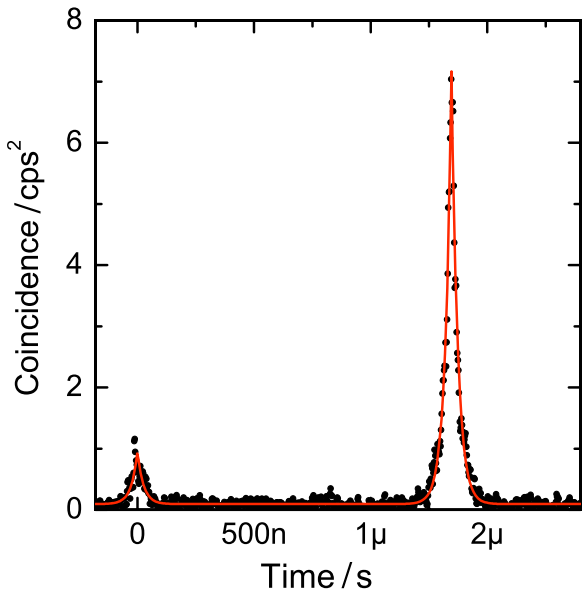

Figure 2. Coincidence histogram of a single NV centre measured by a HBT interferometer.

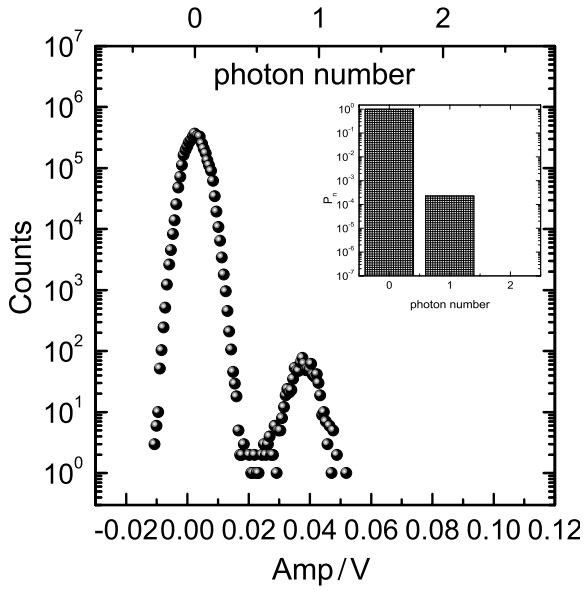

Figure 3. TES histogram of a single NV centre (centre 1).

of the setup. Lower detection efficiencies are simulated by inserting calibrated neutral density filters (NDs) in the optical path [15]. Information on the photon number distribution of the investigated light is gained from the number of 'no-click' events for N different detection efficiencies $\eta_1, \ldots, \eta_N$ in relation to the total number of experimental runs. For a low quantum efficiency, one can expand equation (1) up to the second order in η as (for the derivation, see the appendix)

$$\rho(\eta) = 1 - \eta\langle n\rangle + \tfrac{1}{2}\eta^2\langle n\rangle^2 g^2(0) + \mathrm{O}(\eta^3), \qquad (2)$$

from which the values of the mean photon number $\langle n\rangle$ and of the $g^{(2)}(0)$-value can be obtained using a maximum likelihood estimator or a best fit.

Because the SPS operates in the pulsed excitation mode, the total number of runs is given by the number of laser shots per time interval. In the experiment the number of 'no-click' events is determined within a time frame of 100 s. To suppress photons generated by background radiation between two consecutive laser pulses, the single photon detector is gated. This leads to additional associated fake detection signals occurring less than 2 µs before opening the detection gate. Such spurious events can be inhibited by a gate width of 80 ns as well as an appropriate time delay of 1.33 µs between the open gate time and the sync signal of the pulsed laser using a time delay generator (DG535, Stanford Research). In order to consider the *in situ* transmission of the calibrated ND filters, which varies sensitively with their spatial alignment on the beam path and the wavelength used, we verified the transmission of each filter by absorption measurements using the light coming from the investigated NV centre.

3. Results and discussion

Figure 2 shows the correlation function of a given single NV centre (centre 1) measured by the HBT interferometer. Due to the laser excitation rate of 740 kHz the peaks of the function are clearly separated by regions where no coincidences at all are detected. According to [20, 21] the correlation function consisting of l peaks is fitted by

$$g^{(2)}(t) = A + B \cdot \sum_{j=-1}^{l} \exp\left(-\frac{|t - j \cdot T|}{\tau}\right) - D \cdot \exp\left(-\frac{|t|}{\tau}\right), \qquad (3)$$

where T is the time between two subsequent laser pulses, A is the offset, B is the height of the peaks at non-zero time delay, D is the relative peak reduction of the peak at zero time delay, j is the peak number and τ is the luminescence lifetime of the investigated NV centres, which is calculated to be 26 ns by the fitting procedure. A $g^{(2)}(0) = 0.06 \pm 0.06$ is determined by the ratio $(B - D)/B$, indicating the presence of a single photon emitter. This residual amount of the $g^{(2)}(0)$-value can be attributed to the timing jitter of the SPADs and the background emission from the nano-diamond [21]. A comparable result is determined from the photon number distribution measured by the TES detector, which is pictured in figure 3. The histogram is obtained by counting the number of events with the measured pulse height as a function of the pulse height. The area underneath each peak corresponds to the probability that the detector absorbs no, one or two photons per laser pulse. The $g^{(2)}(0)$-value is then calculated directly from these probabilities:

$$g^{(2)}(0) = \frac{\sum_n (n^2 P_n - n P_n)}{\left(\sum_n n P_n\right)^2}, \qquad (4)$$

where P_n is the probability that n photons strike the surface of the TES detector [22]. For the investigated NV centre, a zero-photon component $P_0 = 99.9 \times 10^{-2}$ and a one-photon component $P_1 = 2.2 \times 10^{-4}$ are determined from the data. Due to the absence of multi-photon components, this gives an estimated experimental value $g^{(2)}(0) = 0.0 + 0.1$, which is comparable to the HBT measurements, see table 1. The

Table 1. Summary of the experimental results obtained by the three measurement techniques.

	TES: photon number components					
	P_0	P_1	P_2	$g^{(2)}_{\mathrm{TES}}(0)$	$g^{(2)}_{\frac{\mathrm{ON}}{\mathrm{OFF}}}(0)$	$g^{(2)}_{\mathrm{HBT}}(0)$
Centre 1	99.9×10^{-2}	2.4×10^{-4}	0	$0.0 + 0.1$	0.02 ± 0.02	0.06 ± 0.06
Centre 2	99.9×10^{-2}	1.1×10^{-3}	3.3×10^{-7}	0.5 ± 0.1	0.5 ± 0.1	0.53 ± 0.06

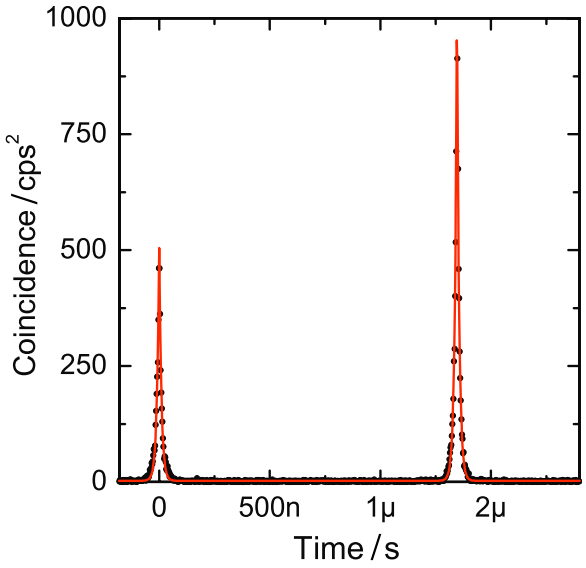

Figure 4. Coincidence histogram of a multi-photon NV centre (centre 2) measured by a HBT interferometer. The luminescence lifetime τ is calculated to be 9.6 ns by the fitting procedure.

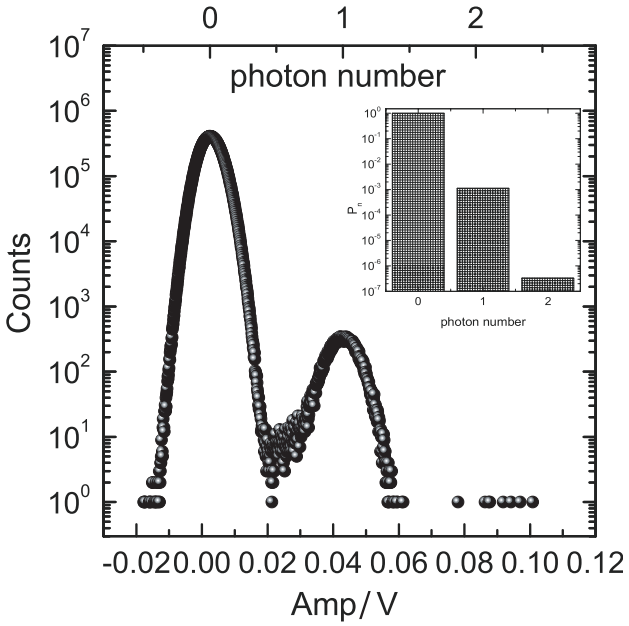

Figure 5. TES histogram of a multi-photon NV centre (centre 2).

measurement uncertainty results here from the uncertainty in the determination of the probabilities of photon number components, see discussion below for centre 2. The latter might also be caused by the low overall efficiency of the whole setup, which is approximately only 0.02% (calculated from the ratio of the probabilities $P_1/(P_1 + P_0)$), thus suppressing significantly multi-photon events due to photon number redistribution.

The experimental data measured by the On/Off technique are fitted by equation (2) considering the overall efficiency of the setup 0.007 ± 0.001, which is experimentally determined by dividing the measured photon count rate by the laser repetition rate. This leads also to a $g^{(2)}(0)$-value of 0.02 ± 0.02. The uncertainty arises from the uncertainty in the determination of the overall efficiency. However, all results for $g^{(2)}(0)$ are compatible with each other, see table 1.

The applicability of the TES and the On/Off methods for the determination of the photon statistics for centres with higher $g^{(2)}(0)$-value was also tested. For centre 2, a significantly higher $g^{(2)}(0)$-value of 0.53 ± 0.06 was measured by the HBT interferometer, see figure 4. This high $g^{(2)}(0)$-value is understood in terms of the presence of a second NV centre contributing to the emission. With the TES, zero-, one- and two-photon probabilities of 0.999, 1.1×10^{-3} and 3.2×10^{-7}, respectively, were observed, see figure 5, resulting in a $g^{(2)}(0)$-value of 0.5 ± 0.1. Analogous to the single photon centre, here the uncertainty of the TES measurements mainly results from the uncertainty in the determination of the probabilities for each photon component. These probabilities are determined from the peak areas in the histogram. As can be seen in figure 5; however, the peaks overlap and exhibit a signicant shoulder, giving rise to an uncertainty.

For the On/Off technique, a $g^{(2)}(0)$-value of 0.5 ± 0.1 was found, determined from an overall efficiency of 0.025 ± 0.005 for the whole setup. Also here, the uncertainty in the overall efficiency determines the uncertainty of the $g^{(2)}(0)$-value. Also here, all techniques for the determination of the $g^{(2)}(0)$-value are practically compatible.

4. Summary

For the purpose of obtaining a standardized metrological characterization of non-classical light emitters, three methods have been applied to study the photon number distribution of a SPS based on the light emitted by NV centres in nano-diamonds. The results from the well known and established HBT interferometric method used to measure the normalized second order intensity correlation function $g^{(2)}(t)$ have been compared with those obtained with photon number resolving TES measurement and with the maximum likelihood assisted reconstruction based on the On/Off detection technique. Concerning the comparison among the $g^{(2)}(0)$ parameters evaluated with the three different methods, we found good agreement in the results, although a high zero photon component is observed. Therefore, further measurements

will be performed investigating NV centres providing brighter emission and higher multi-photon components in order to discuss in detail the applicability of the TES and On/Off methods for the investigation of the photon statistics of single and nearly single photon sources.

Acknowledgments

Acknowledgments to the ERA-NET Plus program, under Grant Agreement No 217257, the Braunschweig International Graduate School of Metrology, the Joint Optical Metrology Center, and the German Federal Ministry of Education and Research, under Grant No 01BL0900 (EPHQUAM: Efficient, compact and controllable Single Photon Sources for Quantum Communication and Metrology).

Appendix

Derivation of equation (2) from equation (1) [23]:

$$\begin{aligned}\rho(\eta) &= \sum_{n=0}^{\infty}(1-\eta)^n\rho_n = \sum_{n=0}^{\infty}\sum_{k=0}^{n}\binom{n}{k}(-\eta)^k\rho_n \\ &= \sum_{k=0}^{\infty}\sum_{n=k}^{n}\binom{n}{k}(-\eta)^k\rho_n \\ &= \sum_{n=0}^{\infty}\rho_n - \eta\sum_{n=1}^{\infty}n\rho_n + \frac{1}{2}\eta^2\sum_{n=2}^{\infty}n(n-1)\rho_n + \mathrm{O}(\eta^3).\end{aligned} \tag{A.1}$$

For pulsed excitation it is appropriate to define a normalized photon correlation function as follows.

With the electric field density operator

$$\rho = \sum_{m,n}\rho_{m,n}|m\rangle\langle n|,$$

the second order correlation function $g^{(2)}(0)$ can be rewritten as

$$g^{(2)}(0) = \frac{\langle n(n-1)\rangle}{\langle n^2\rangle}.$$

Inserting this $g^{(2)}(0)$-value into equation (A.1) one can obtain

$$\rho(\eta) = 1 - \eta\langle n\rangle + \frac{1}{2}\eta^2\langle n\rangle^2 g^{(2)}(0) + \mathrm{O}(\eta^3).$$

References

[1] Alleaume R, Treussart F, Messin G, Dumeige Y, Roch J-F, Beveratos A, Brori-Tualle R, Poizat J-P and Grangier P 2004 *New J. Phys.* **6** 92
[2] Beveratos A, Brouri R, Gacio T, Villing A, Poizat J-P and Grangier P 2002 *Phys. Rev. Lett.* **89** 187901
[3] Waks E, Inoue I, Santori C, Fattal D, Vuckovic J, Solomon G and Yamamoto Y 2002 *Nature* **420** 762
[4] O'Brien J-L 2007 *Science* **318** 1567
[5] Beaumont A, Cheung J Y and Chunnilall C J 2009 *Nucl. Instrum. Methods Phys. Res.* A **610** 183
[6] Cheung J Y, Migdall A and Rastello M L 2009 *J. Mod. Opt.* **56** 139
[7] Schmunk W, Rodenberger M, Peters S, Hofer H and Kück S 2011 *J. Mod. Opt.* **58** 14
[8] Braig C, Zarda P, Kurtsiefer C and Weinfurter H 2003 *Appl. Phys.* B **76** 113
[9] Cheung J Y, Chunnilall C J, Woolliams E R, Mountford N P F J R, Wang J and Thomas P J 2007 *J. Mod. Opt.* **54** 373
[10] Zwinkels J C, Ikonen E, Fox N P, Ulm G and Rastello M L 2010 *Metrologia* **47** R15
[11] Hadfield R H 2009 *Nature Photon.* **3** 696
[12] Lolli L, Taralli E, Portesi C, Alberto D, Rajteri M and Monticone E 2011 *IEEE Trans. Appl. Supercond.* **21** 215
[13] Taralli E, Portesi C, Lolli L, Monticone E, Rajteri M, Novikov I and Beyer J 2010 *Supercond. Sci. Technol.* **23** 105012
[14] Avenhaus M, Coldenstrodt-Ronge H B, Laiho K, Mauerer W, Walmsley I A and Silberhorn C 2008 *Phys. Rev. Lett.* **101** 053601
[15] Rossi A R, Olivares S and Paris M G A 2004 *Phys. Rev.* A **70** 055801
Zambra G, Andreoni A, Bondani M, Gramegna M, Genovese M, Brida G, Rossi A and Paris M G A 2005 *Phys. Rev. Lett.* **95** 063602
[16] Brida G, Genovese M, Gramegna M, Meda A, Piacentini F, Traina P, Predazzi E, Olivares S and Paris M G A 2011 *Adv. Sci. Lett.* **4** 1
[17] Breitenbach G, Schiller S and Mlynik J 1997 *Nature* **387** 471
[18] Quantum Communications Victoria (http://qcvictoria.com)
[19] Portesi C, Taralli E, Rocci R, Rajteri M and Monticone E 2008 *J. Low Temp. Phys.* **151** 12
[20] Weston K D, Dyck M, Tinnefeld P, Müller C, Herten D P and Sauer M 2002 *Anal. Chem.* **74** 5342
[21] Han K Y, Willig K I, Rittweger E, Jelezko F, Eggeling C and Hell S W 2009 *Nano Lett.* **9** 3323
[22] Walls D F and Milburn G J 2008 *Quantum Optics* 2nd edn (Berlin: Springer)
[23] Rossi A R and Paris M G A 2005 *Eur. Phys. J.* D **32** 223